

1 **Service life of some HDPE geomembranes**

2

3 Fernando Luiz Lavoie^{1*}, Marcelo Kobelnik¹, Clever Aparecido Valentin¹, Maria de
4 Lurdes Lopes², Ennio Marques Palmeira³, Jefferson Lins da Silva¹

5

6 ¹São Carlos School of Engineering, University of São Paulo-USP, São Paulo 13566-
7 590, Brazil; mkobelnik@gmail.com (M.K.); cclever@sc.usp.br (C.A.V.);
8 jefferson@sc.usp.br (J.L.d.S.)

9 ²CONSTRUCT-GEO, Department of Civil Engineering, University of Porto; Porto
10 4200-465, Portugal; lcosta@fe.up.pt (M.d.L.L.)

11 ³University of Brasília, Department of Civil and Environmental Engineering, 70910-900
12 Brasília, DF, Brazil, palmeira@unb.br (E.M.P.)

13 *Corresponding Author: fernando.lavoie@usp.br (F.L.L.); Tel.: +55-119-8105-8718,
14 ORCID: 0000-0003-1242-3708

15

16 **Abstract.** This study evaluated nine exhumed high-density polyethylene (HDPE)
17 geomembranes from different Brazilian civil construction facilities under several
18 exposure times, from two to fifteen years in service. Physical and thermal analyses were
19 performed to understand the behavior of the geomembranes' samples in the final
20 condition after the environmental exposure and, in some cases, also after contact with
21 residues. The analyses showed the vulnerability of the geomembranes investigated and
22 demonstrated, in general, the short-term durability of the products tested. Finally, this
23 research showed the need to standardize the resins and additives types of the

24 geomembranes to guarantee their long-term durability, avoiding detrimental
25 environmental impacts and associated financial costs.

26

27 **Keywords:** geomembrane; HDPE; durability; final condition; service life

28

29 **1 Introduction**

30 Geomembranes are applied in environmental, geotechnical and transportation facilities.

31 High-density polyethylene (HDPE) geomembranes are the most widely used liner
32 elements in the world. In facilities such as water ponds, waste liquid ponds, leachate
33 ponds, farm ponds, canals and artificial beaches, the aging mechanisms act on the whole
34 geomembrane's service life, at least for the slope crest part above the water table (Rollin
35 and Rigo 1991; Vertematti 2015; Palmeira 2018; Koerner 2005).

36 The service life of HDPE geomembranes can reach more than a century or less than a
37 decade. It depends on the material composition and the field's boundary conditions. Many
38 factors command the material's long-term performance, such as field temperature,
39 mechanical stresses during construction, local stress concentration, covered or protected
40 conditions, contact with residues, resin quality and product formulation (Rowe and
41 Sangam 2002; Zhang et al. 2018; Peggs and Zanzinger 2018).

42 Lifetime is usually defined as the time to reduce a given material's property to 50 % of
43 its virgin value. However, this is an arbitrary method to determine the product's lifetime.

44 The end of life is when the geomembrane can no longer perform the fluid containment
45 function. For the end-of-life prediction, the designer needs experience, extrapolation of
46 the measured properties, or laboratory testing to simulate and accelerate the field
47 conditions (Peggs and Zanzinger 2018; Rowe 2012; Rowe 2020).

48 According to Rowe (2012), when the geomembrane can no longer be considered effective
49 in working as a barrier element, the leakage is controlled by the liner layer under the
50 geomembrane. In this condition, the material reached its service life and the stress
51 cracking commands the process, culminating in a considerable increase of defects in the
52 geomembrane.

53 The decrease in the geomembrane's service life can happen due to the exposure to high
54 temperatures, accelerating the oxidative degradation and, consequently, causing losses in
55 stress crack resistance. For HDPE geomembranes, manufacturers do not recommend
56 exposure to temperatures higher than 57 °C (Rowe and Rimal 2009; Rowe et al. 2010).

57 Jafari et al. (2014) reported monitoring the landfill temperature in six cell composite liners.

58 The authors could predict the HDPE geomembrane service life through a three-stage
59 degradation model. They used stress crack resistance, tensile break resistance and tensile
60 break elongation as parameters for the study. However, the authors considered stress
61 crack resistance as the determinant for end of life. The service life results presented a
62 range of between 960 years to 20 years, depending on the measured temperature in the
63 cells.

64 Gulec et al. (2004) estimated the antioxidant depletion of a 1.5 mm-thick HDPE
65 geomembrane after exposure to synthetic acidic mine drainage for 22 months at 60 °C,
66 40 °C and 20 °C. The antioxidant depletion estimation was 426 years to 46 years. The
67 melt flow index (MFI) results demonstrated an increasing trend.

68 Rowe et al. (2009) analyzed an HDPE geomembrane with 2.0 mm of nominal thickness
69 for 10 years immersed in synthetic leachate, water and air at different temperatures.

70 According to the authors, using a three-stage degradation model, the sample in contact
71 with the leachate had a service life of more than 50 years at 50 °C.

72 The service life of an HDPE geomembrane applied in a double liner landfill was evaluated
73 by Rowe and Hoor (2009). Considering a liner configuration of a primary HDPE
74 geomembrane, a geosynthetic clay liner (GCL), 1 m of soil foundation or compacted clay
75 liner (CCL) and a secondary HDPE geomembrane, the service life of the secondary
76 geomembrane was estimated in 75 years at 50 °C.

77 This work evaluated the service life of nine high-density polyethylene smooth
78 geomembranes exhumed from different Brazilian civil construction facilities subjected to
79 different exposure times. Physical and thermal analyses were performed to understand
80 the behavior of the geomembranes' samples in the final condition after the environmental
81 exposure and, in some cases, also after contact with residues.

82

83 **2 Material and Methods**

84 **2.1 Materials**

85 The HDPE geomembrane samples collected in the field and evaluated in this work are
86 described in Table 1. The samples were exhumed from different Brazilian construction
87 works in many applications. Lavoie (2021) analyzed the final condition of these samples
88 using physical and thermal analyses. The samples' characterization was described by
89 Lavoie et al. (2020; 2020-1; 2021; 2021-1; 2022).

90 The samples were collected directly from the sites. Geomembrane samples MIN, MIN2,
91 LDO, CAM, CAM1 and CAM2 were stored in a covered place without contamination
92 right after the collection until the transportation to the laboratory. Otherwise, the CLIQ
93 and LCH samples were left uncovered in the field for 2 months before transportation to
94 the laboratory. Finally, the sample LTE was left for 1 week uncovered in the field before
95 being transported to the laboratory.

96 **2.2 Performed Laboratory Tests**

97 **2.2.1 Melt Flow Index (MFI) Test**

98 The melt flow index (MFI) test (ASTM D 1238, 2020) was carried out using a plastometer
99 manufactured by Instron at Norwood, USA, model CEAST MF20. The material was
100 extruded through a smooth bore (2.095 ± 0.005 mm in diameter and 8000 ± 0.025 mm
101 long) at 190 ± 0.08 °C with a 5.0 ± 0.01 kg of deadweight. After 10 min (with precision
102 of 1 s) of the sample extrusion, the material mass was measured using an analytical
103 balance with 0.0001 g of precision.

104

105 **2.2.2 Tensile Properties**

106 The tensile test (ASTM D 6693, 2020) was performed using a universal machine
107 manufactured by EMIC in São José dos Pinhais, Brazil, model DL 3000, with a 2-kN load
108 cell, conducted with a test speed of 50 ± 1 mm min⁻¹ and the type IV dog bone specimen.
109 The tensile strength and tensile elongation were recorded for the material's machine
110 direction.

111

112 **2.2.3 Stress Crack Resistance (SCR) Test**

113 The stress crack resistance (SCR) was determined using a deadweight load of 30 % of the
114 yield tensile strength of the samples (precision of 10 g) and a notch of 20 % of the
115 specimen thickness (precision of 0.001 mm). The test (ASTM D 5397, 2020) was
116 performed using equipment manufactured by WT Indústria at São Carlos, Brazil. The
117 specimens were immersed in a solution with 10 ± 0.1 % of Igepal CO 630 and 90 ± 0.1 %
118 of water at a constant temperature of 50 ± 1 °C. The results were reported using the mean
119 rupture time of 5 specimens with a precision of 1 s.

120 **2.2.4 Oxidative-Induction Time (OIT) Tests**

121 This study utilized two tests to determine the oxidative-induction time (OIT) of the HDPE
122 geomembrane samples. The standard OIT (Std. OIT) (ASTM D 3895, 2019) and the high-
123 pressure OIT (HP OIT) (ASTM D 5885, 2020) tests were performed. Both tests can
124 search for the different antioxidants in the material's blend. DSC (differential scanning
125 calorimetry) equipment was used to perform the tests, model Q20, manufactured by TA
126 Instruments in New Castle, USA, using a sample mass of 5 ± 0.5 mg inside an aluminum
127 crucible. The standard OIT test was performed at 200 ± 2 °C with an oxygen constant
128 pressure of 140 ± 5 kPa, a heating rate of 20 ± 1 °C min⁻¹ and a flow rate of 50 ± 5 mL
129 min⁻¹. The high-pressure OIT test was conducted at 150 ± 0.5 °C with an oxygen constant
130 pressure of 3.4 ± 0.06 MPa and a heating rate of 20 ± 1 °C min⁻¹.

131

132 **3 Results and Discussion**

133 **3.1 MFI Test Results**

134 The MFI is an excellent parameter to compare virgin with exposed samples. The increase
135 or decrease in this index can explain possible polymer degradation (Telles et al. 1984).
136 Table 2 presents the MFI test results and the standard deviations (SD) for the analyzed
137 exhumed samples. Figure 1 shows the exhumed samples' MFI results versus exposure
138 time (log scale), including the tendency line of the results. The oldest samples (LDO,
139 MIN2, CAM, and CAM1) presented the highest MFI values (near or higher than 1.0 g 10
140 min⁻¹). The highlight was the CAM1 sample, which was exhumed from the Shrimp
141 Farming Pond's slope liner and continuously exposed to environmental agents, which
142 presented the highest MFI value and needed to be tested at a lower temperature (160 °C)
143 due to its atypical behavior, showing the highest standard deviation among the tested

144 samples. The tendency line indicates the MFI's increase with the exposure time. The
145 Coefficient of Determination (R^2) of the tendency line was 0.1049, which demonstrated
146 a high data variation.

147

148 **3.2 Tensile Test Results**

149 Tables 3 and 4 present, respectively, the tensile resistance and elongation at break test
150 results, including the standard deviations (SD) for the analyzed exhumed samples.

151 Figures 2 and 3 show, respectively, the tensile resistance versus exposure time (log scale)
152 and the tensile elongation versus exposure time for the exhumed samples, including the
153 tendency lines of the results. In Figure 2, the 100 % value represents the minimum value
154 required according to GRI-GM13 (2021) for each thickness. Only the LCH and LTE
155 samples presented higher tensile resistance than the minimum tensile resistance value
156 prescribed by the American standard. The tendency line presents an almost constant
157 behavior close to 90 % of the retained tensile resistance. The Coefficient of Determination
158 (R^2) of the tendency line was 0.0001, which demonstrated a high data variation. For the
159 tensile elongation results (Figure 3), only the LCH sample presented a value of elongation
160 at break higher than 700 %. It is important to note that the LCH sample was the thickest
161 exhumed sample, presenting the best mechanical behavior. The CLIQ, MIN, MIN2, LDO,
162 and CAM2 samples exhibited brittle behavior for some test specimens tested. Three
163 samples (CAM2, MIN, and LDO) presented average tensile elongation values lower than
164 350 %, which corresponds to less than 50 % of the minimum required value according to
165 GRI-GM13 (2021). The worst tensile behavior was verified for the LDO sample, which
166 is the oldest analyzed sample. A high standard deviation was noted for the CLIQ, MIN,
167 MIN2, LDO and CAM2 samples, demonstrating that polymer changes are occurring. The

168 tendency line indicates the tensile elongation's decrease along the exposure time. The
169 Coefficient of Determination (R^2) of the tendency line was 0.0455, which also
170 demonstrates a high data variation.

171

172 **3.3 Stress Crack Resistance Test Results**

173 Table 5 presents the stress crack resistance (SCR) test results, including the standard
174 deviations (SD) for the analyzed exhumed samples. Figure 4 shows the stress crack
175 resistance results versus exposure time (log scale) for the exhumed samples, including
176 the tendency line of the results. The minimum SCR value required by GRI-GM13 (2021)
177 is 500 h. The CAM, CLIQ, and LCH samples presented SCR values higher than the
178 minimum value prescribed by the American standard. The other samples showed SCR
179 values lower than 100 h, especially LDO and CAM1, the oldest analyzed samples, which
180 exhibited very low SCR values, and this can affect their liner performance. The CAM and
181 CAM1 samples, although exhumed from the same shrimp farming pond, showed opposite
182 SCR results due to the environmental exposure experienced by the CAM1 sample. The
183 tendency line indicates the stress crack resistance's decrease along the exposure time,
184 reaching less than 200 h for 15 years of exposure. A high standard deviation was noted
185 for the CLIQ, LCH and CAM samples, particularly for LCH. The Coefficient of
186 Determination (R^2) of the tendency line was 0.0323, revealing a high data variation.

187

188 **3.4 Oxidative-Induction Time (OIT) Test Results**

189 Tables 6 and 7 present Std. OIT and HP OIT test results, respectively, including the
190 standard deviations (SD) for the analyzed exhumed samples. Figures 5 and 6 show,
191 respectively, the Std. OIT and HP OIT test results versus exposure time (log scale) for
192 the exhumed samples, including the tendency line for the results.

193 The minimum Std. OIT value required by GRI-GM13 (2021) is 100 min. The LCH
194 sample was the only exhumed geomembrane that presented a Std. OIT value higher than
195 100 min. The CAM2, LTE, and CLIQ samples presented Std. OIT values higher than 50
196 min (50 % of the minimum required value by the American standard). The LDO, CAM,
197 CAM1 and MIN2 samples, the oldest samples, presented near or lower Std. OIT values
198 than 10 min (10 % of the minimum required value by the American standard). The
199 tendency line indicates the Std. OIT's decrease along the exposure time, almost reaching
200 the total antioxidant consumption after 15 years. A high standard deviation was noted for
201 the CLIQ sample. The Coefficient of Determination (R^2) of the tendency line was 0.4503,
202 also revealing a high data variation.

203 The minimum HP OIT value required by GRI-GM13 (2021) is 400 min. None of the
204 tested samples presented OIT-HP values equal to or higher than 400 min. The presence
205 of HALS (Hindered Amine Light Stabilizer) in the additive package increases the OIT-
206 HP results. As this test is performed at 150 °C, probably none of the virgin samples
207 presented HALS in their additive package. The best performance was that of the thicker
208 sample (LCH). The CLIQ, LTE, and CAM2 samples presented HP OIT values higher
209 than 150 min (37.5 % of the minimum required value by the American standard). The
210 MIN, MIN2, and LDO samples presented HP OIT values higher than 100 min (25 % of
211 the minimum required value by the American standard). The CAM and CAM1 samples,
212 from the same shrimp farming pond liner, presented different results. The CAM1 sample,
213 which was exhumed from the slope liner, presented oxidation immediately after the
214 oxidation process started in the test, that is, the antioxidant content was completely
215 depleted. This result is due to the type of exposure of the CAM1 sample, which was
216 submitted to weather exposure for 8.25 years. The tendency line indicates the HP OIT's

217 decrease with the exposure time, reaching less than 100 min after 15 years. A high
218 standard deviation was noted for the MIN2 and CAM2 samples. The Coefficient of
219 Determination (R^2) of the tendency line was 0.03395, which demonstrated a high data
220 variation.

221

222 **3.5 Behavior of the Exhumed Samples**

223 Table 8 shows the behavior of the samples from the analysis of their property's values,
224 including the thermal analyses performed by Lavoie (2020; 2020-1; 2021; 2021-1; 2022).

225 It was observed that the antioxidant depletion is related to the geomembrane's thickness,
226 that is, the thicker sample, LCH, presented the highest Std. OIT value. Otherwise, the
227 CAM, CAM1, LDO, MIN2 samples presented the lowest Std. OIT values.

228 Some exhumed samples showed different changes in thermal behavior due to the
229 environmental agents and the contact with the residues along the exposure time. The LCH
230 sample, which was in contact with leachate, was the sample that presented the greatest
231 thermal changes. Other samples also presented significant changes in the thermal
232 behavior, such as the LDO, CAM2, CLIQ and LTE samples.

233 High MFI values (low viscosity) were noted for the MIN2, LDO, CAM and CAM1
234 samples. On the other hand, the CLIQ, LCH, LTE, MIN and CAM2 samples presented
235 low MFI values.

236 Some exhumed samples showed brittle behavior (MIN, LDO and CAM2 samples), and
237 the CLIQ and MIN2 samples presented some tendency to brittle behavior. The loss of
238 ductility has a high impact on the geomembrane's performance.

239 The SCR results demonstrated low values for the exhumed samples compared to the GRI-
240 GM13 (2021) requirements. The LTE, MIN, MIN2, LDO, CAM1 and CAM2 samples

241 presented the tendency to brittle failure. Only the CLIQ, LCH and CAM samples
242 demonstrated high SCR results.

243

244 **4 Conclusions**

245 This work aimed to understand the final conditions of nine exhumed HDPE smooth
246 geomembranes applied in some geotechnical and environmental Brazilian facilities.

247 The analyzed exhumed geomembranes showed several changes in their properties, except
248 for the LCH sample, the thicker one, which presented good performance in the physical
249 properties, but some changes in thermal decomposition. The LTE sample changes its
250 physical properties over time and could yield to a liner rupture in the near future. The
251 MIN, MIN2, LDO, and CAM2 samples showed brittle tensile behavior, low SCR values,
252 low Std. OIT values and could culminate in a system failure. The CAM1 sample presented
253 an atypical viscosity, low SCR result, unprotection from the additives against the
254 oxidative degradation, certainly having reached its lifetime. The CLIQ and CAM samples
255 changed their physical and thermal behavior and may cause liner rupture in the short-
256 term. The evaluated tendency lines demonstrated high variations, which limits the
257 extrapolation of results.

258 The exhumed samples analyses showed the vulnerability of the HDPE geomembranes
259 tested and demonstrated, in general, the short-term durability of the products tested.

260 Finally, this research showed the need for a standardization of resins and additives of the
261 HDPE geomembranes to guarantee products with long-term durability, avoiding losses in
262 terms of environmental impacts and financial costs. Better quality control practices of
263 geosynthetic products must be required by designers and enforced by regulatory agencies

264 to avoid using inadequate products regarding their service lives and required engineering
265 properties.

266

267 Credit Authorship Statement: Conceptualisation, F.L.L., M.K. and C.A.V.; methodology,
268 F.L.L., M.K. and C.A.V.; validation, F.L.L., M.K., C.A.V., J.L.d.S., M.d.L.L. and
269 E.M.P.; formal analysis, F.L.L., M.K. and C.A.V.; investigation, F.L.L., M.K. and
270 C.A.V.; resources, F.L.L., M.K. and J.L.d.S.; data curation, F.L.L., M.K. and C.A.V.;
271 writing—original draft preparation, F.L.L., M.K. and C.A.V.; writing—review and
272 editing, F.L.L., J.L.d.S., M.d.L.L. and E.M.P.; visualisation, F.L.L., M.K., C.A.V.,
273 J.L.d.S., M.d.L.L. and E.M.P.; supervision, F.L.L. and J.L.d.S.; project administration,
274 F.L.L. and J.L.d.S.; funding acquisition, F.L.L. and J.L.d.S. All authors have read and
275 agreed to the published version of the manuscript.

276

277 **Funding:** This research received no external funding.

278 **Institutional Review Board Statement:** Not applicable.

279 **Informed Consent Statement:** Not applicable.

280 **Declaration of interests:** The authors declare that they have no known competing financial
281 interests or personal relationships that could have appeared to influence the work reported
282 in this paper.

283

284 **References**

285 ASTM (American Society for Testing and Materials). ASTM D 1238 Standard Test
286 Methods for Melt Flow Rates of Thermoplastics by Extrusion Plastometer; ASTM: West
287 Conshohocken, PA, USA, 2020; p. 17.

288 ASTM (American Society for Testing and Materials). ASTM D 3895 Standard Test
289 Method for Oxidative-Induction Time of Polyolefins by Differential Scanning
290 Calorimetry; ASTM: West Conshohocken, PA, USA, 2019; p. 7.

291 ASTM (American Society for Testing and Materials). ASTM D 5397 Standard Test
292 Method for Evaluation of Stress Crack Resistance of Polyolefin Geomembranes Using
293 Notched Constant Tensile Load Test; ASTM: West Conshohocken, PA, USA, 2020; p.
294 7.

295 ASTM (American Society for Testing and Materials). ASTM D 5885 Standard Test
296 Method for Oxidative Induction Time of Polyolefin Geosynthetics by High-Pressure
297 Differential Scanning Calorimetry; ASTM: West Conshohocken, PA, USA, 2020; p. 5.

298 ASTM (American Society for Testing and Materials). ASTM D 6693 Standard Test
299 Methods for Determining Tensile Properties of Nonreinforced Polyethylene and
300 Nonreinforced Flexible Polypropylene Geomembranes; ASTM: West Conshohocken, PA,
301 USA, 2020; p. 5.

302 GRI—GM13: Test methods, test properties and testing frequency for high-density
303 polyethylene (HDPE) smooth and textured geomembranes SM. Geosynthetic Institute,
304 2021.

305 Gulec, S.B.; Edil, T.B.; Benson, C.H.; Effect of acidic mine drainage on the polymer
306 properties of an HDPE geomembrane. *Geosynth. Int.* 2004, 11 (2), 60–72. Doi:
307 10.1680/gein.2004.11.2.60.

308 Jafari, N.H.; Stark, T.D.; Rowe, R.K. Service Life of HDPE Geomembranes subjected to
309 elevated temperatures. *J. Hazard. Toxic Radioact. Waste* 2014, 18, 16–26. Doi:
310 10.1061/(ASCE)HZ.2153-5515.0000188.

311 Koerner, R.M., *Designing with Geosynthetics*. Englewood Cliffs, Prentice Hall Publ.

312 Co., New Jersey, 2005.

313 Lavoie, F.L. Study on the durability of HDPE geomembranes applied to geotechnics and
314 the environment using laboratory aged samples and in situ exhumed samples. Doctor
315 dissertation – São Carlos School of Engineering, University of São Paulo, São Carlos,
316 2021.

317 Lavoie, F.L.; Kobelnik, M.; Valentin, C.A.; Lins da Silva, J.; de Lurdes Lopes, M. Study
318 of an exhumed HDPE geomembrane used in an industrial water pond: physical and
319 thermoanalytical characterisations, *Results Mater* 8 2020, 100131, Doi:
320 10.1016/j.rinma.2020.100131.

321 Lavoie, F.L.; Kobelnik, M.; Valentin, C.A.; Lins da Silva, J.; de Lurdes Lopes, M. HDPE
322 geomembranes for environmental protection: two case studies, *Sustainability* 12 2020-1,
323 <https://doi.org/10.3390/su12208682>, 20, 8682.

324 Lavoie, F.L.; Kobelnik, M.; Valentin, C.A.; da Silva Tirelli, É.F.; Lins da Silva, J.; de
325 Lurdes Lopes, M. Environmental Protection with HDPE Geomembranes in Mining
326 Facility Constructions. *Constr. Mater.* 2021, 1, 122-133. Doi:
327 10.3390/constrmater1020009.

328 Lavoie, F.L.; Kobelnik, M.; Valentin, C.A.; da Silva Tirelli, É.F.; Lins da Silva, J.; de
329 Lurdes Lopes, M. Environmental protection liner in a biodegradable waste pond: A case
330 study. *Case Stud. Chem. Environ. Eng.* 2021-1, 4, 100133. Doi:
331 10.1016/j.cscee.2021.100133.

332 Lavoie, F.L.; Kobelnik, M.; Valentin, C.A.; da Silva Tirelli, É.F.; Lins da Silva, J.; de
333 Lurdes Lopes, M. Evaluation of exhumed HDPE geomembranes used as a liner in
334 Brazilian shrimp farming ponds. *Case Stud. Constr. Mater.* 2022, 16, e00809. Doi:
335 10.1016/j.cscm.2021.e00809.

336 Peggs, I.D.; Zanzinger, H. Technical notes from the Berlin 2 HDPE geomembrane
337 workshop: assessing remaining service life, 2018.

338 Rollin, A.R.; Rigo, J.M. Geomembranes - Identification and Performance Testing, 1st
339 ed., Chapman and Hall: London, 1991.

340 Rowe, R.K.; Sangam, H.P. Durability of HDPE geomembranes. *Geotext Geomembr.*
341 2002, 20, 77–95. Doi: 10.1016/S0266-1144(02)00005-5.

342 Rowe, R.K.; Rimal, S.; Sangam, H.P. Ageing of HDPE geomembrane exposed to air,
343 water and leachate at different temperatures. *Geotext. Geomembr.* 2009, 27 (2), 137–151.
344 Doi: 10.1016/j.geotextmem.2008.09.007.

345 Rowe, R.K.; Hoor, A. Predicted temperatures and service lives of secondary
346 geomembrane landfill liners. *Geosynth. Int.* 2009, 16 (2), 71–82. Doi:
347 10.1680/gein.2009.16.2.71.

348 Rowe, R.K.; Hoor, A.; Pollard, A. Numerical examination of a method for reducing the
349 temperature of municipal solid waste landfill liners. *J. Environ. Eng.* 2010, 136 (8), 794–
350 803. Doi: 10.1061/(ASCE)EE.1943-7870.0000212.

351 Rowe, R.K. Short- and long-term leakage through composite liners. The 7th Arthur
352 Casagrande Lecture. *Can. Geotech. J.* 2012, 49(2) 141–169. Doi: 10.1139/t11-092.

353 Rowe, R.K. Protecting the Environment with Geosynthetics: 53rd Karl Terzaghi Lecture.
354 *Geotech Geoenviron.* 2020, 146(9), 04020081. Doi: 10.1061/(ASCE)GT.1943-
355 5606.0002239.

356 Telles, R.W.; Lubowitz, H.R.; Unger, S.L. Assessment of environmental stress corrosion
357 of polyethylene liners in landfills and impoundments. 1st ed. Cincinnati: U.S. EPA, 1984.

358 Vertematti J.C.: *Manual Brasileiro de Geossintéticos*. Blücher, São Paulo, 2015.

359 Palmeira E.M.: Geossintéticos em Geotecnia e Meio Ambiente. Oficina de Textos, São
360 Paulo, 2018.

361 Zhang, L.; Bouazza, A.; Rowe, R. K.; Scheirs, J. Effects of a very low pH solution on the
362 properties of an HDPE geomembrane. Geosynth. Int. 2018, 25, 118-131. Doi:
363 10.1680/jgein.17.00037.

364

365 **Table Captions:**

366 **Table 1:** HDPE geomembrane exhumed samples used in this research

367 **Table 2:** MFI test results of the exhumed samples

368 **Table 3:** Tensile resistance at break test results of the exhumed samples

369 **Table 4:** Tensile elongation at break test results of the exhumed samples

370 **Table 5:** SCR test results of the exhumed samples

371 **Table 6:** Std. OIT test results of the exhumed samples

372 **Table 7:** HP OIT test results of the exhumed samples

373 **Table 8:** Exhumed samples' behavior

374

375 **Figure Captions:**

376 **Figure 1:** MFI results versus exposure time for the exhumed samples

377 **Figure 2:** Retained tensile resistance at break results versus exposure time for the
378 exhumed samples

379 **Figure 3:** Tensile elongation at break results versus exposure time for the exhumed
380 samples

381 **Figure 4:** SCR results versus exposure time for the exhumed samples

382 **Figure 5:** Std. OIT results versus exposure time for the exhumed samples

383 **Figure 6:** HP OIT results versus exposure time for the exhumed samples

384

385 Table 1. HDPE geomembrane exhumed samples used in this research

Sample	Nominal Thickness (mm)	Application	Exposure Time (years)
CLIQ [15]	1.0	Industrial Water Pond	2.25
LTE [16]	1.0	Sewage Treatment Aeration Pond	2.75
LCH [16]	2.0	Municipal Landfill Leachate Pond	5.17
MIN [17]	1.0	Pond for Water Use for the Iron Ore Process	7.92
MIN2 [17]	1.0	Spillway Channel of a Ferronickel Tailing Dam	10.08
LDO [18]	0.8	Biodegradable Waste Pond	15.17
CAM [19]	0.8	Shrimp Farming Pond – Bottom Liner	8.25
CAM1 [19]	0.8	Shrimp Farming Pond – Slope Liner	8.25
CAM2 [19]	0.8	Another Shrimp Farming Pond	3.0

386

387 Table 2. MFI test results of the exhumed samples

Sample	Exposure Time (years)	MFI (g 10 min ⁻¹)	SD (g 10 min ⁻¹)
CLIQ	2.25	0.4256	0.0079
LTE	2.75	0.4555	0.0061
LCH	5.17	0.5008	0.0072
MIN	7.92	0.4016	0.0052
MIN2	10.08	0.8635	0.0229
LDO	15.17	0.7375	0.0225
CAM	8.25	1.4191	0.0325
CAM1	8.25	3.9939	0.2188
CAM2	3.0	0.5831	0.1380

388

389

390

391

392

393

394

395

396

397 Table 3. Tensile resistance at break test results of the exhumed samples

Sample	Exposure Time (years)	Tensile Resistance (kN m ⁻¹)	SD (kN m ⁻¹)
CLIQ	2.25	21.98	6.82
LTE	2.75	27.12	1.30
LCH	5.17	60.40	7.66
MIN	7.92	22.11	4.05
MIN2	10.08	24.14	4.30
LDO	15.17	20.35	0.98
CAM	8.25	19.23	3.11
CAM1	8.25	16.12	2.09
CAM2	3.0	16.37	2.15

398

399 Table 4. Tensile elongation at break test results of the exhumed samples

Sample	Exposure Time (years)	Tensile Elongation (%)	SD (%)
CLIQ	2.25	482.63	329.65
LTE	2.75	679.33	27.53
LCH	5.17	752.60	81.38
MIN	7.92	301.15	397.19
MIN2	10.08	495.52	445.38
LDO	15.17	259.24	342.71
CAM	8.25	684.63	96.46
CAM1	8.25	627.07	63.27
CAM2	3.0	312.74	335.42

400

401 Table 5. SCR test results of the exhumed samples

Sample	Exposure Time (years)	SCR (h)	SD (h)
CLIQ	2.25	709.45	78.63
LTE	2.75	30.89	12.31
LCH	5.17	542.15	508.17
MIN	7.92	45.25	34.13
MIN2	10.08	20.22	7.04
LDO	15.17	8.89	4.12
CAM	8.25	1151.98	44.64
CAM1	8.25	4.25	1.52
CAM2	3.0	90.41	17.01

402

403 Table 6. Std. OIT test results of the exhumed samples

Sample	Exposure Time (years)	Std. OIT (min)	SD (min)
CLIQ	2.25	53.27	10.86
LTE	2.75	60.69	0.21
LCH	5.17	110.70	1.56
MIN	7.92	29.55	4.70
MIN2	10.08	10.86	5.60
LDO	15.17	6.94	1.04
CAM	8.25	6.36	0.52
CAM1	8.25	9.65	0.70
CAM2	3.0	67.61	5.13

404 Table 7. HP OIT test results of the exhumed samples

Sample	Exposure Time (years)	HP OIT (min)	SD (min)
CLIQ	2.25	162.55	7.42
LTE	2.75	180.00	1.41
LCH	5.17	231.50	2.12
MIN	7.92	110.45	5.87
MIN2	10.08	113.25	12.37
LDO	15.17	106.45	5.87
CAM	8.25	60.60	4.81
CAM1	8.25	0	0
CAM2	3.0	166.05	15.06

405

406 Table 8. Exhumed samples' behavior

Sample	Viscosity	SCR Behavior	Tensile Behavior	Antioxidant Depletion	Thermal Behavior
CLIQ	High	High	TBB	High	CB; OVL
LCH	High	High	Ductile	Low	CTD; CB; INT
LTE	High	TBF	Ductile	Low	INT
MIN	High	TBF	BB	High	Normal
MIN2	Low	TBF	TBB	ATAC	Normal
LDO	Low	TBF	BB	ATAC	OVL; INT
CAM	Low	High	Ductile	ATAC	BCE
CAM1	Low	TBF	Ductile	ATAC	BCE
CAM2	High	TBF	BB	Low	BCE; CTD

407 ATAC – Almost total antioxidant consumption

408 BB – Brittle behavior

409 BCE – Baseline change event

410 CB – Combustion

411 CTD – Changes in thermal decomposition

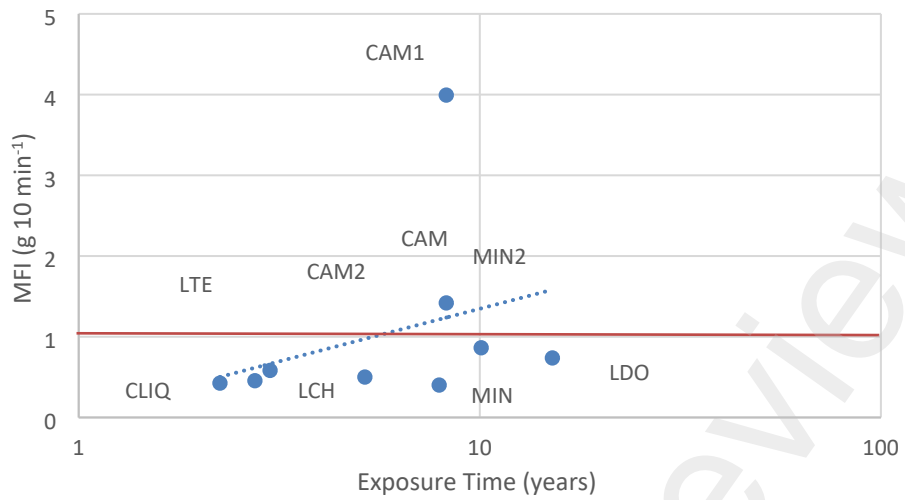
412 INT – Interaction between the polymer and the solution

413 OVL – Overlapped reactions

414 TBB – Tendency to brittle behavior

415 TBF – Tendency to brittle failure

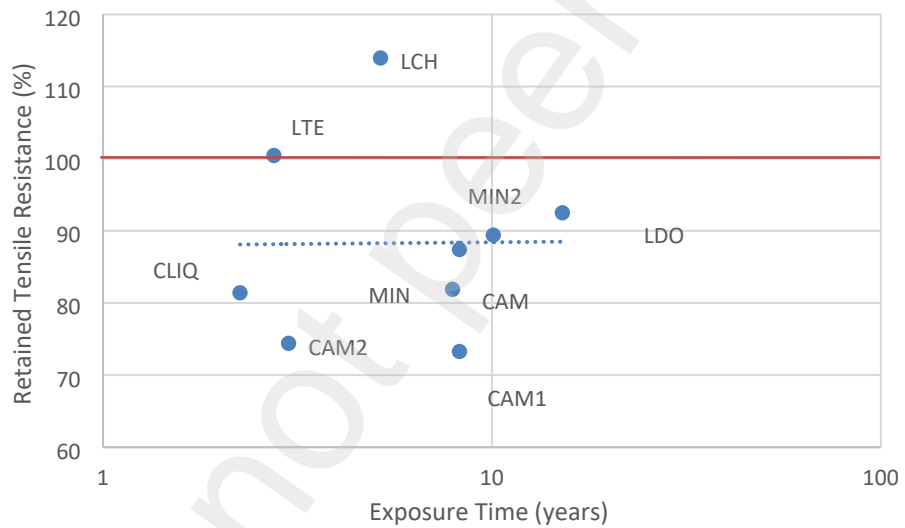
416



417

418 Figure 1. MFI results versus exposure time for the exhumed samples

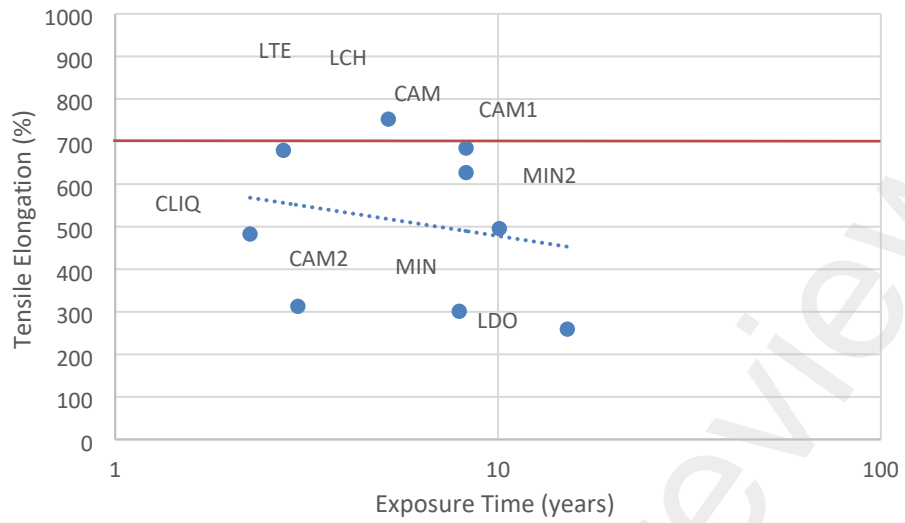
419



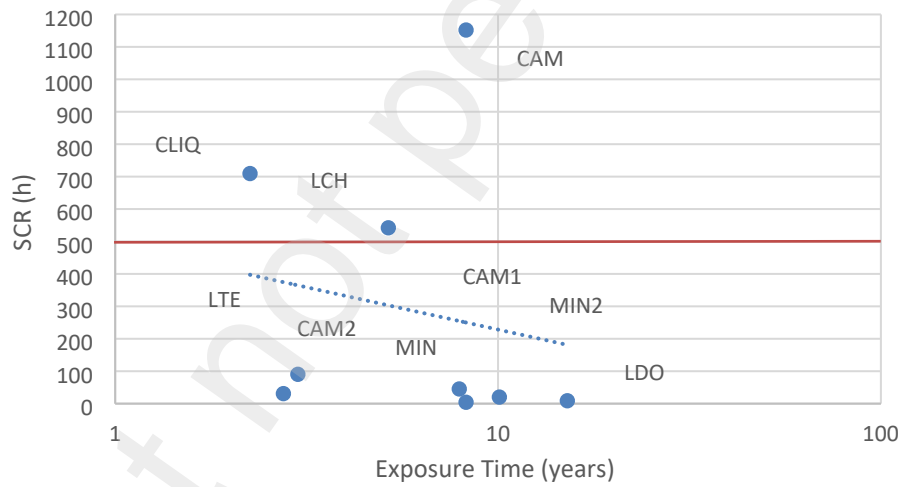
420

421 Figure 2. Retained tensile resistance at break results versus exposure time for the
 422 exhumed samples

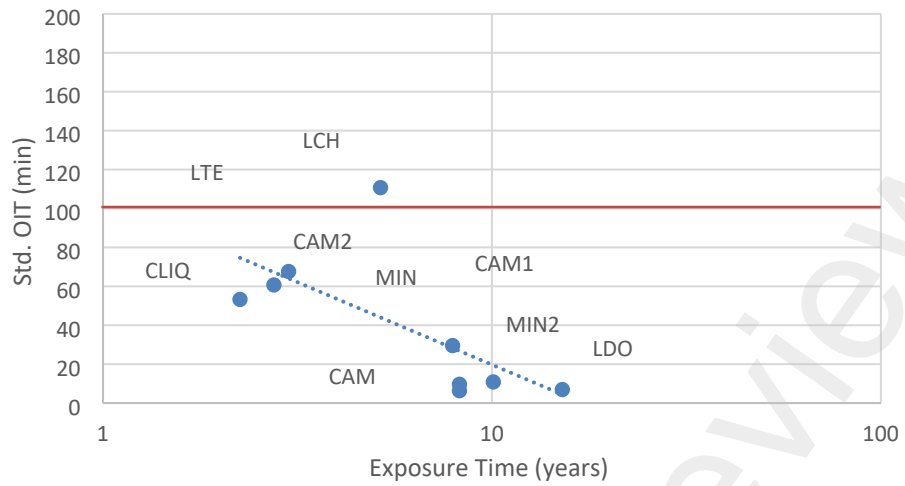
423



424
 425 Figure 3. Tensile elongation at break results versus exposure time for the exhumed
 426 samples
 427
 428



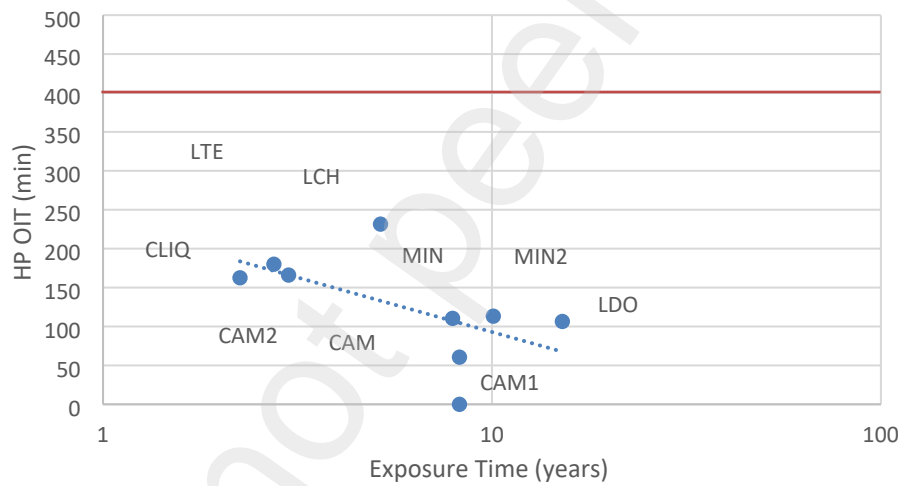
429
 430 Figure 4. SCR results versus exposure time for the exhumed samples
 431



432

433 Figure 5. Std. OIT results versus exposure time for the exhumed samples

434



435

436 Figure 6. HP OIT results versus exposure time for the exhumed samples

437